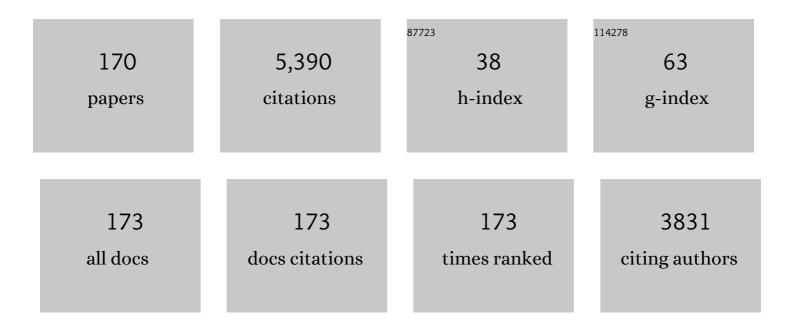
## Alfred Leipertz

List of Publications by Year in descending order

Source: https://exaly.com/author-pdf/10707800/publications.pdf Version: 2024-02-01



#	Article	IF	CITATIONS
1	Density, Refractive Index, Interfacial Tension, and Viscosity of Ionic Liquids [EMIM][EtSO <sub>4</sub> ], [EMIM][NTf <sub>2</sub> ], [EMIM][N(CN) <sub>2</sub> ], and [OMA][NTf <sub>2</sub> ] in Dependence on Temperature at Atmospheric Pressure. Journal of Physical Chemistry B, 2008, 112, 12420-12430.	1.2	302
2	Experimental Vibrational Study of Imidazolium-Based Ionic Liquids: Raman and Infrared Spectra of 1-Ethyl-3-methylimidazolium Bis(Trifluoromethylsulfonyl)imide and 1-Ethyl-3-methylimidazolium Ethylsulfate. Applied Spectroscopy, 2007, 61, 1306-1311.	1.2	281
3	The role of the C2 position in interionic interactions of imidazolium based ionic liquids: a vibrational and NMR spectroscopic study. Physical Chemistry Chemical Physics, 2010, 12, 14153.	1.3	278
4	Two-dimensional soot-particle sizing by time-resolved laser-induced incandescence. Optics Letters, 1995, 20, 2342.	1.7	161
5	Performance characteristics of soot primary particle size measurements by time-resolved laser-induced incandescence. Applied Optics, 1998, 37, 5647.	2.1	127
6	Density, Surface Tension, and Kinematic Viscosity of Hydrofluoroethers HFE-7000, HFE-7100, HFE-7200, HFE-7300, and HFE-7500. Journal of Chemical & Engineering Data, 2015, 60, 3759-3765.	1.0	127
7	Viscosity, Interfacial Tension, Density, and Refractive Index of Ionic Liquids [EMIM][MeSO <sub>3</sub> ], [EMIM][MeOHPO <sub>2</sub> ], [EMIM][OcSO <sub>4</sub> ], and [BBIM][NTf <sub>2</sub> ] in Dependence on Temperature at Atmospheric Pressure. Journal of Chemical & amp: Engineering Data, 2009, 54, 2576-2583.	1.0	116
8	Soot temperature measurements and implications for time-resolved laser-induced incandescence (TIRE-LII). Combustion and Flame, 2000, 120, 439-450.	2.8	111
9	Development of an algebraic reaction rate closure for the numerical calculation of turbulent premixed methane, ethylene, and propane/air flames for pressures up to 1.0 MPa. Combustion and Flame, 2005, 140, 257-266.	2.8	111
10	Experimental comparison of single-shot broadband vibrational and dual-broadband pure rotational coherent anti-Stokes Raman scattering in hot air. Applied Optics, 1996, 35, 2665.	2.1	93
11	Concentrationâ€Dependent Hydrogenâ€Bonding Effects on the Dimethyl Sulfoxide Vibrational Structure in the Presence of Water, Methanol, and Ethanol. ChemPhysChem, 2010, 11, 630-637.	1.0	80
12	Flame front detection and characterization using conditioned particle image velocimetry (CPIV). Optics Express, 2007, 15, 15444.	1.7	78
13	Measurement of the resolved flame structure of turbulent premixed flames with constant reynolds number and varied stoichiometry. Proceedings of the Combustion Institute, 1998, 27, 785-792.	0.3	77
14	Densities and Excess Molar Volumes for Binary Mixtures of Ionic Liquid 1-Ethyl-3-methylimidazolium Ethylsulfate with Solvents. Journal of Chemical & Engineering Data, 2010, 55, 4068-4074.	1.0	77
15	Simultaneous two-dimensional flow velocity and gas temperature measurements by use of a combined particle image velocimetry and filtered Rayleigh scattering technique. Applied Optics, 2001, 40, 5379.	2.1	70
16	Viscosity, Interfacial Tension, Self-Diffusion Coefficient, Density, and Refractive Index of the Ionic Liquid 1-Ethyl-3-methylimidazolium Tetracyanoborate as a Function of Temperature at Atmospheric Pressure. Journal of Chemical & Engineering Data, 2012, 57, 828-835.	1.0	68
17	Gas-phase temperature measurement in the vaporizing spray of a gasoline direct-injection injector by use of pure rotational coherent anti-Stokes Raman scattering. Optics Letters, 2004, 29, 247.	1.7	66
18	Revealing the Influence of the Strength of Coulomb Interactions on the Viscosity and Interfacial Tension of Ionic Liquid Cosolvent Mixtures. Journal of Physical Chemistry B, 2007, 111, 12817-12822.	1.2	64

#	Article	IF	CITATIONS
19	Molecular interactions and macroscopic effects in binary mixtures of an imidazolium ionic liquid with water, methanol, and ethanol. Journal of Molecular Structure, 2012, 1018, 45-53.	1.8	64
20	Laser-induced breakdown flame thermometry. Combustion and Flame, 2012, 159, 3576-3582.	2.8	63
21	Application of a beam homogenizer to planar laser diagnostics. Optics Express, 2006, 14, 10171.	1.7	62
22	Picosecond time-resolved pure-rotational coherent anti-Stokes Raman spectroscopy for N_2 thermometry. Optics Letters, 2009, 34, 3755.	1.7	61
23	Application of 266-nm and 355-nm Nd:YAG laser radiation for the investigation of fuel-rich sooting hydrocarbon flames by Raman scattering. Applied Optics, 2004, 43, 5564.	2.1	60
24	Determination of Primary Particle Size Distributions from Time-Resolved Laser-Induced Incandescence Measurements. Applied Optics, 2004, 43, 3726.	2.1	55
25	Solute solubility as criterion for the appearance of amorphous particle precipitation or crystallization in the supercritical antisolvent (SAS) process. Journal of Supercritical Fluids, 2012, 66, 350-358.	1.6	52
26	Quantitative Analysis of Alphaâ€∢scp>Dâ€glucose in an Ionic Liquid by Using Infrared Spectroscopy. ChemPhysChem, 2008, 9, 1317-1322.	1.0	51
27	Viscosity of Diisodecyl Phthalate by Surface Light Scattering (SLS). Journal of Chemical & Engineering Data, 2007, 52, 1803-1810.	1.0	50
28	Acetone laser-induced fluorescence behavior for the simultaneous quantification of temperature and residual gas distribution in fired spark-ignition engines. Applied Optics, 2010, 49, 37.	2.1	50
29	Manipulating the size, the morphology and the polymorphism of acetaminophen using supercritical antisolvent (SAS) precipitation. Journal of Supercritical Fluids, 2013, 82, 230-237.	1.6	49
30	Condensation heat transfer on single horizontal smooth and finned tubes and tube bundles for R134a and propane. International Journal of Heat and Mass Transfer, 2013, 56, 516-524.	2.5	47
31	Simultaneous vibrational and pure rotational coherent anti-Stokes Raman spectroscopy for temperature and multispecies concentration measurements demonstrated in sooting flames. Applied Optics, 2002, 41, 564.	2.1	46
32	Combined shifted-excitation Raman difference spectroscopy and support vector regression for monitoring the algal production of complex polysaccharides. Analyst, The, 2013, 138, 5639.	1.7	46
33	Simultaneous temperature and exhaust-gas recirculation-measurements in a homogeneous charge-compression ignition engine by use of pure rotational coherent anti-Stokes Raman spectroscopy. Applied Optics, 2006, 45, 3646.	2.1	45
34	Study of the influence of electric fields on flames using planar LIF and PIV techniques. Proceedings of the Combustion Institute, 2011, 33, 3195-3201.	2.4	44
35	One-dimensional, time-resolved Raman measurements in a sooting flame made with 355-nm excitation. Applied Optics, 1998, 37, 4937.	2.1	43
36	An Industrial Reference Fluid for Moderately High Viscosity. Journal of Chemical & Engineering Data, 2008, 53, 2003-2011.	1.0	43

#	Article	IF	CITATIONS
37	Direct determination of the turbulent flux by simultaneous application of filtered rayleigh scattering thermometry and particle image velocimetry. Proceedings of the Combustion Institute, 2002, 29, 2669-2677.	2.4	42
38	Laser-induced fluorescence of ketones at elevated temperatures for pressures up to 20 bars by using a 248 nm excitation laser wavelength: experiments and model improvements. Applied Optics, 2006, 45, 4982.	2.1	40
39	Combined coherent anti-Stokes Raman spectroscopy and linear Raman spectroscopy for simultaneous temperature and multiple species measurements. Optics Letters, 2006, 31, 1908.	1.7	39
40	On the effect of ionic wind on structure and temperature of laminar premixed flames influenced by electric fields. Combustion and Flame, 2017, 176, 391-399.	2.8	37
41	Experimental comparison of broadband rotational coherent anti-Stokes Raman scattering (CARS) and broadband vibrational CARS in a flame. Optics Letters, 1984, 9, 341.	1.7	36
42	Effect of Fuel Properties on Spray Breakup and Evaporation Studied for a Multihole Direct Injection Spark Ignition Injector. Energy & Fuels, 2010, 24, 4341-4350.	2.5	35
43	Simultaneous temperature and relative nitrogen–oxygen concentration measurements in air with pure rotational coherent anti-Stokes Raman scattering for temperatures to as high as 2050 K. Applied Optics, 1997, 36, 3500.	2.1	34
44	Measurement of the conditioned turbulence and temperature field of a premixed Bunsen burner by planar laser Rayleigh scattering and stereo particle image velocimetry. Experiments in Fluids, 2005, 39, 375-384.	1.1	34
45	Mutual diffusion in binary mixtures of ionic liquids and molecular liquids by dynamic light scattering (DLS). Physical Chemistry Chemical Physics, 2011, 13, 9525.	1.3	34
46	Demonstration of a signal enhanced fast Raman sensor for multiâ€species gas analyses at a low pressure range for anesthesia monitoring. Journal of Raman Spectroscopy, 2015, 46, 708-715.	1.2	34
47	Two-dimensional temperature determination in the exhaust region of a laminar flat-flame burner with linear Raman scattering. Applied Optics, 1997, 36, 6989.	2.1	33
48	Direct evaluation of the subgrid scale scalar flux in turbulent premixed flames with conditioned dual-plane stereo PIV. Proceedings of the Combustion Institute, 2009, 32, 1723-1730.	2.4	33
49	High resolution dual-plane stereo-PIV for validation of subgrid scale models in large-eddy simulations of turbulent premixed flames. Combustion and Flame, 2009, 156, 1552-1564.	2.8	33
50	Gas phase temperature measurements in the liquid and particle regime of a flame spray pyrolysis process using O <sub>2</sub> -based pure rotational coherent anti-Stokes Raman scattering. Applied Optics, 2012, 51, 6063.	0.9	33
51	A new guarded parallel-plate instrument for the measurement of the thermal conductivity of fluids and solids. International Journal of Heat and Mass Transfer, 2013, 58, 610-618.	2.5	32
52	Systematic experiments on turbulent premixed Bunsen flames including turbulent flux measurements. Combustion and Flame, 2008, 152, 616-631.	2.8	31
53	Improvement of Condensation Heat Transfer by Surface Modifications. Heat Transfer Engineering, 2008, 29, 343-356.	1.2	31
54	Parameter study on the performance of dropwise condensation. International Journal of Thermal Sciences, 1998, 37, 539-548.	0.2	30

#	Article	IF	CITATIONS
55	Characterization of Nano-Particles Using Laser-Induced Incandescence. Particle and Particle Systems Characterization, 2003, 20, 81-93.	1.2	30
56	Application of an optical pulse stretcher to coherent anti-Stokes Raman spectroscopy. Optics Letters, 2004, 29, 2381.	1.7	30
57	Quantitative analysis of the near-wall mixture formation process in a passenger car direct-injection Diesel engine by using linear Raman spectroscopy. Applied Optics, 2005, 44, 6606.	2.1	30
58	Element by element prediction model of condensation heat transfer on a horizontal integral finned tube. International Journal of Heat and Mass Transfer, 2013, 62, 463-472.	2.5	30
59	Sound velocity measurements by the use of dynamic light scattering: data reduction by the application of a Fourier transformation. Applied Optics, 1993, 32, 3886.	2.1	28
60	On the role of physiochemical properties on evaporation behavior of DISI biofuel sprays. Experiments in Fluids, 2013, 54, 1.	1.1	28
61	Deconvolution of Raman spectra for the quantification of ternary highâ€pressure phase equilibria composed of carbon dioxide, water and organic solvent. Journal of Raman Spectroscopy, 2014, 45, 246-252.	1.2	28
62	Infrared Spectroscopy of a Wilkinson Catalyst in a Roomâ€Temperature Ionic Liquid. ChemPhysChem, 2008, 9, 2207-2213.	1.0	27
63	Characterization of Escherichia coli suspensions using UV/Vis/NIR absorption spectroscopy. Analytical Methods, 2010, 2, 123-128.	1.3	27
64	Pure rotational coherent anti-Stokes Raman scattering: comparison of evaluation techniques for determining single-shot simultaneous temperature and relative N_2–O_2 concentration. Applied Optics, 1998, 37, 5659.	2.1	26
65	Determination of Glucose and Cellobiose Dissolved in the Ionic Liquid 1-Ethyl-3-Methylimidazolium Acetate Using Fourier Transform Infrared Spectroscopy. Applied Spectroscopy, 2009, 63, 1041-1049.	1.2	26
66	On the Characteristics of Ion Implanted Metallic Surfaces Inducing Dropwise Condensation of Steam. Langmuir, 2010, 26, 5971-5975.	1.6	26
67	Hybrid femtosecond/picosecond coherent antiâ€Stokes Raman scattering for highâ€speed CH <sub>4</sub> /N <sub>2</sub> measurements in binary gas mixtures. Journal of Raman Spectroscopy, 2013, 44, 1336-1343.	1.2	26
68	Fuel property and fuel temperature effects on internal nozzle flow, atomization and cyclic spray fluctuations of a direct injection spark ignition–injector. International Journal of Engine Research, 2013, 14, 543-556.	1.4	26
69	Simultaneous and time-resolved temperature and relative CO_2–N_2 and O_2–CO_2–N_2 concentration measurements with pure rotational coherent anti-Stokes Raman scattering for pressures as great as 5 MPa. Applied Optics, 2005, 44, 5582.	2.1	25
70	Non-invasive quantification of phase equilibria of ternary mixtures composed of carbon dioxide, organic solvent and water. Journal of Supercritical Fluids, 2013, 84, 146-154.	1.6	25
71	Transient electric field response of laminar premixed flames. Proceedings of the Combustion Institute, 2013, 34, 3303-3310.	2.4	25
72	Determination of the dynamic viscosity of transparent fluids by using dynamic light scattering. Applied Optics, 1993, 32, 3813.	2.1	24

#	Article	IF	CITATIONS
73	Gas mixing analysis by simultaneous Raman imaging and particle image velocimetry. Optics Letters, 2009, 34, 3122.	1.7	24
74	Laser sheet dropsizing based on two-dimensional Raman and Mie scattering. Applied Optics, 2009, 48, 1853.	2.1	24
75	Vibrational structure of the polyunsaturated fatty acids eicosapentaenoic acid and arachidonic acid studied by infrared spectroscopy. Journal of Molecular Structure, 2010, 965, 121-124.	1.8	24
76	Influence of electric fields on premixed laminar flames: Visualization of perturbations and potential for suppression of thermoacoustic oscillations. Proceedings of the Combustion Institute, 2015, 35, 3521-3528.	2.4	24
77	Industrial combustion control using UV emission tomography. Proceedings of the Combustion Institute, 1996, 26, 2869-2875.	0.3	23
78	Simultaneous temperature and relative O_2–N_2 concentration measurements by single-shot pure rotational coherent anti-Stokes Raman scattering for pressures as great as 5 MPa. Applied Optics, 2000, 39, 6918.	2.1	23
79	Spray/wall interaction influences on the diesel engine mixture formation process investigated by spontaneous Raman scattering. Proceedings of the Combustion Institute, 2002, 29, 617-623.	2.4	22
80	Time-resolved measurement of the local equivalence ratio in a gaseous propane injection process using laser-induced gratings. Optics Express, 2006, 14, 12994.	1.7	22
81	High-speed CH planar laser-induced fluorescence imaging using a multimode-pumped optical parametric oscillator. Optics Letters, 2011, 36, 3927.	1.7	22
82	Two-dimensional Raman mole-fraction and temperature measurements for hydrogen-nitrogen mixture analysis. Applied Optics, 2009, 48, B57.	2.1	21
83	Binary Diffusion Coefficients for Mixtures of Ionic Liquids [EMIM][N(CN) <sub>2</sub> ], [EMIM][NTf <sub>2</sub> ], and [HMIM][NTf <sub>2</sub> ] with Acetone and Ethanol by Dynamic Light Scattering (DLS). Journal of Physical Chemistry B, 2013, 117, 2429-2437.	1.2	21
84	A Raman spectroscopic method for the determination of high pressure vapour liquid equilibria. Fluid Phase Equilibria, 2013, 360, 265-273.	1.4	21
85	Two-dimensional direct measurement of the turbulent flux in turbulent premixed swirl flames. Proceedings of the Combustion Institute, 2007, 31, 1337-1344.	2.4	20
86	Investigation of CO2 sorption in molten polymers at high pressures using RamanÂline imaging. Polymer, 2013, 54, 812-818.	1.8	20
87	Characterization of four potential laser-induced fluorescence tracers for diesel engine applications. Applied Optics, 2013, 52, 8001.	0.9	20
88	LOCALLY RESOLVED INVESTIGATION OF THE VAPORIZATION OF GDI SPRAYS APPLYING DIFFERENT LASER TECHNIQUES. , 2006, 16, 319-330.		20
89	Simultaneous temperature and relative oxygen and methane concentration measurements in a partially premixed sooting flame using a novel CARS-technique. Journal of Molecular Structure, 2003, 661-662, 515-524.	1.8	19
90	Tracer-based laser-induced fluorescence measurement technique for quantitative fuel/air-ratio measurements in a hydrogen internal combustion engine. Applied Optics, 2008, 47, 6488.	2.1	19

#	Article	IF	CITATIONS
91	Development of a simplified dual-pump dual-broadband coherent anti-Stokes Raman scattering system. Applied Optics, 2009, 48, B43.	2.1	19
92	Simultaneous laser-induced fluorescence and Raman imaging inside a hydrogen engine. Applied Optics, 2009, 48, 6643.	2.1	19
93	Determination of Physicochemical Parameters of Ionic Liquids and Their Mixtures with Solvents Using Laser-Induced Gratings. Journal of Physical Chemistry B, 2011, 115, 8528-8533.	1.2	19
94	Characterization of a CH planar laser-induced fluorescence imaging system using a kHz-rate multimode-pumped optical parametric oscillator. Applied Optics, 2012, 51, 2589.	0.9	19
95	Quantification of the mass transport in a two phase binary system at elevated pressures applying Raman spectroscopy: Pendant liquid solvent drop in a supercritical carbon dioxide environment. International Journal of Heat and Mass Transfer, 2013, 62, 729-740.	2.5	19
96	Simultaneous Measurement of Speed of Sound, Thermal Diffusivity, and Bulk Viscosity of 1-Ethyl-3-methylimidazolium-Based Ionic Liquids Using Laser-Induced Gratings. Journal of Physical Chemistry B, 2014, 118, 14493-14501.	1.2	19
97	Determination of probe volume dimensions in coherent measurement techniques. Applied Optics, 2008, 47, 6601.	2.1	18
98	In situ optical monitoring of the solution concentration influence on supercritical particle precipitation. Journal of Supercritical Fluids, 2010, 55, 282-291.	1.6	18
99	Investigation of the chemical stability of the laser-induced fluorescence tracers acetone, diethylketone, and toluene under IC engine conditions using Raman spectroscopy. Applied Optics, 2013, 52, 6300.	0.9	18
100	Pilot Injection Ignition Properties Under Low-Temperature, Dilute In-Cylinder Conditions. SAE International Journal of Engines, 0, 6, 1888-1907.	0.4	18
101	Microfluidic investigation into mass transfer in compressible multi-phase systems composed of oil, water and carbon dioxide at elevated pressure. Journal of Supercritical Fluids, 2013, 84, 121-131.	1.6	17
102	Observation of liquid solution volume expansion during particle precipitation in the supercritical CO2 antisolvent process. Journal of Supercritical Fluids, 2011, 56, 121-124.	1.6	16
103	Thermophysical Properties of a Quaternary Refrigerant Mixture: Comparison of Dynamic Light Scattering Measurements with a Simple Prediction Method. International Journal of Thermophysics, 2007, 28, 743-757.	1.0	15
104	Photonenkorrelationsspektroskopie. Physik in Unserer Zeit, 1984, 15, 68-75.	0.0	14
105	Dropwise Condensation Heat Transfer on Plasma-Ion-Implanted Small Horizontal Tube Bundles. Heat Transfer Engineering, 2010, 31, 821-828.	1.2	14
106	Thermal diffusivity and sound velocity of Round-Robin R134a. Fluid Phase Equilibria, 1996, 125, 245-255.	1.4	13
107	Simultaneous application of single-shot Ramanography and particle image velocimetry. Optics Letters, 2006, 31, 1005.	1.7	13
108	Entwicklung eines Echtzeitanalyse-Systems zur Charakterisierung von Brenngasgemischen in Gasturbinenkraftwerken. Chemie-Ingenieur-Technik, 2011, 83, 247-253.	0.4	13

#	Article	IF	CITATIONS
109	Simultaneous Raman and elastic light scattering imaging for particle formation investigation. Optics Letters, 2010, 35, 2553.	1.7	12
110	Lycopene solubility in mixtures of carbon dioxide and ethyl acetate. Journal of Supercritical Fluids, 2013, 75, 6-10.	1.6	12
111	Light scattering by surface waves on a vertical layer of liquid toluene. Applied Optics, 1997, 36, 7615.	2.1	11
112	Determination of several thermophysical properties of toluene using a single experimental setup. Fluid Phase Equilibria, 1999, 161, 337-351.	1.4	11
113	Diffusion Measurements in Fluids by Dynamic Light Scattering. , 2005, , 579-618.		11
114	Application of laser-induced incandescence to suspended carbon black particles. Optics Letters, 2007, 32, 1947.	1.7	11
115	Injection of ethanol into supercritical CO_2: Determination of mole fraction and phase state using linear Raman scattering. Optics Express, 2007, 15, 8377.	1.7	11
116	Raman mixture composition and flow velocity imaging with high repetition rates. Optics Express, 2010, 18, 24579.	1.7	11
117	Application of linear Raman spectroscopy for the determination of acetone decomposition. Optics Express, 2011, 19, 11052.	1.7	11
118	Simultaneous two-dimensional measurement of fuel–air ratio and temperature in a direct-injection spark-ignition engine using a new tracer-pair laser-induced fluorescence technique. International Journal of Engine Research, 2016, 17, 120-128.	1.4	11
119	Nutzung von Laser-Raman-Verfahren in der Verbrennungstechnik. Chemie-Ingenieur-Technik, 1989, 61, 39-48.	0.4	10
120	Dynamic light scattering system with a novel scattering cell for the measurement of particle diffusion coefficients. Review of Scientific Instruments, 1996, 67, 3164-3169.	0.6	10
121	Einsatz PTFE-Ĥnlicher Hartstoff-schichten bei der Tropfenkondensation von Wasserdampf. Chemie-Ingenieur-Technik, 1997, 69, 122-125.	0.4	10
122	A-priori testing of an eddy viscosity model for the density-weighted subgrid scale stress tensor in turbulent premixed flames. Experiments in Fluids, 2010, 49, 839-851.	1.1	10
123	In situ monitoring of the acetylene decomposition and gas temperature at reaction conditions for the deposition of carbon nanotubes using linear Raman scattering. Optics Express, 2010, 18, 18223.	1.7	10
124	Flow field characterization in a vertically oriented cold wall CCVD reactor by particle image velocimetry. Chemical Engineering Journal, 2012, 184, 315-325.	6.6	10
125	Laserbasierte On-line-Analyse von Biogasen mit einer Raman-Sonde. TM Technisches Messen, 2014, 81, 546-553.	0.3	10
126	Giant-pulsed laser Raman oxygen measurements in a premixed laminar methane–air flame. Applied Optics, 1985, 24, 4509.	2.1	9

#	Article	IF	CITATIONS
127	On the Mechanism of Dropwise Condensation of Steam on Ion Implanted Metallic Surfaces. Journal of Heat Transfer, 2010, 132, .	1.2	9
128	Investigation of Fuel Effects on Spray Atomization and Evaporation Studied for a Multi-hole DISI Injector with a Late Injection Timing. SAE International Journal of Fuels and Lubricants, 0, 5, 254-264.	0.2	9
129	Simultaneous in situ Raman monitoring of the solid and gas phases during the formation and growth of carbon nanostructures inside a cold wall CCVD reactor. Carbon, 2014, 78, 164-180.	5.4	9
130	Laserâ€Ramanâ€Spektroskopie in der WĤne―und StrĶmungstechnik. Physik in Unserer Zeit, 1981, 12, 107-1	1 <b>5.</b> 0	8
131	Contact-free measurements of oxygen concentration in industrial flames by raman scattering. Chemical Engineering and Technology, 1987, 10, 190-203.	0.9	8
132	Thermophysical properties of fluids by light scattering. Fluid Phase Equilibria, 1996, 125, 219-233.	1.4	8
133	Fuel concentration imaging inside an optically accessible diesel engine using 1-methylnaphthalene planar laser-induced fluorescence. International Journal of Engine Research, 2014, 15, 741-750.	1.4	8
134	Simultaneous imaging of fuel vapor mass fraction and gas-phase temperature inside gasoline sprays using two-line excitation tracer planar laser-induced fluorescence. Applied Optics, 2016, 55, 1453.	2.1	8
135	J3 Dropwise Condensation. , 2010, , 933-938.		8
136	Influence of the fuel quantity on the spray formation and ignition under current engine relevant conditions. , 2011, , .		7
137	In Situ Raman Monitoring of the Formation and Growth of Carbon Nanotubes via Chemical Vapor Deposition. Procedia Engineering, 2015, 102, 190-200.	1.2	7
138	CH and NO planar laser-induced fluorescence and Rayleigh-scattering in turbulent flames using a multimode optical parametric oscillator. Applied Optics, 2021, 60, 98.	0.9	7
139	Experimental Investigation Of Small Single And Multiple Free Jets By Laser Raman Spectroscopy. Optical Engineering, 1979, 18, .	0.5	6
140	Raman oxygen detection for combustion control and regulation. Applied Optics, 1983, 22, 901.	2.1	6
141	Two-photon stimulated Raman excitation of thermal laser-induced gratings in molecular gases using broadband radiation of a single laser. Optics Express, 2008, 16, 18379.	1.7	6
142	Studies on the Origin of Dropwise Condensation of Steam on Ion Implanted Metallic Surfaces. Chemie-Ingenieur-Technik, 2011, 83, 545-551.	0.4	6
143	Giant Pulse Laser Raman Probe For Low Gas Concentration Detection. Optical Engineering, 1981, 20, 599.	0.5	5
144	Gas Sensor for Volatile Anesthetic Agents Based on Raman Scattering. Physics Procedia, 2012, 39, 835-842.	1.2	5

#	Article	IF	CITATIONS
145	Quantitative DISI Spray Vapor Temperature Study for Different Biofuels by Two-Line Excitation Laser-Induced Fluorescence. , 2012, , .		5
146	12th International Congress of Engine Combustion Processes: Current problems and modern techniques (ENCOM2015). International Journal of Engine Research, 2016, 17, 3-5.	1.4	5
147	Messung der TemperaturleitfĤigkeit transparenter Flļssigkeiten mit Hilfe der Photonenkorrelationsspektroskopie. Chemie-Ingenieur-Technik, 1984, 56, 334-335.	0.4	4
148	Locally Resolved Measurement of Gas-Phase Temperature and EGR-Ratio in an HCCI-Engine and Their Influence on Combustion Timing. , 2007, , .		4
149	Measurement and Prediction of the Thermal Conductivity of Ionic Liquids. Chemie-Ingenieur-Technik, 2011, 83, 1510-1514.	0.4	4
150	Raman Processes and their Application. , 1989, , 107-122.		4
151	Laserspektroskopische Bestimmung thermophysikalischer Eigenschaften transparenter Fluide. Chemie-Ingenieur-Technik, 1992, 64, 17-24.	0.4	3
152	Laser Diagnostics for the Model Development in Turbulent Premixed Flames. Zeitschrift Fur Physikalische Chemie, 2009, 223, 481-502.	1.4	3
153	Simultaneous quantitative Acetone-PLIF measurements for determination of temperature and gas composition fields in an IC-engine. Physics Procedia, 2010, 5, 689-696.	1.2	3
154	Broadband Two-Color Laser-Induced Incandescence Pyrometry Approach for Nanoparticle Characterization with Improved Sensitivity. Applied Spectroscopy, 2013, 67, 1098-1100.	1.2	3
155	Visualisation of Temperature and Vapour Distribution in a Gasoline Spray. MTZ Worldwide, 2014, 75, 50-55.	0.1	3
156	Influence of the wall on the combustion and pollutant formation in small bore DI diesel engines. MTZ Worldwide, 2005, 66, 25-28.	0.1	1
157	Chapter 6 Time-Resolved Laser-Induced Incandescence. Advances in Chemical Engineering, 2009, , 223-269.	0.5	1
158	Attenuated Total Reflection Infrared Difference Spectroscopy (ATR-IRDS) for Quantitative Reaction Monitoring. Applied Spectroscopy, 2012, 66, 685-688.	1.2	1
159	Nutzung von Laser-Streulicht-Techniken in der WÄ <b>¤</b> me-, StrĶmungs- und Verfahrenstechnik. , 1990, , 387-393.		1
160	Laseroptische Charakterisierung von gasgetragenen Nanoteilchen mit der zeitaufgelösten laserinduzierten Glühtechnik (TIRE-LII) (Laser-Optical Characterization of Air-Borne Nanoparticles by) Tj ETQqO	0 <b>0.</b> æBT	Oværlock 10
161	Combustion and pollutant formation in diesel engines. MTZ Worldwide, 2008, 69, 48-55.	0.1	0

Experimental Study on the Origin of Dropwise Condensation of Steam on Ion Implanted Metallic Surfaces. , 2010, , . 162

0

#	Article	IF	CITATIONS
163	Raman Difference Spectroscopy Approach for Monitoring of a Bioreactor. , 2012, , .		0
164	Raman Analytics for Complex Liquid Phase Systems. , 2014, , .		0
165	13th International Congress of Engine Combustion Processes: Current Problems and Modern Techniques (ENCOM2017). International Journal of Engine Research, 2018, 19, 3-6.	1.4	0
166	Tropfenkondensation. Springer Reference Technik, 2018, , 1-7.	0.0	0
167	Development of Imaging Laser Diagnostics for the Validation of LE-Simulations of Flows with Heat and Mass Transfer. Notes on Numerical Fluid Mechanics and Multidisciplinary Design, 2009, , 175-184.	0.2	0
168	J3 Tropfenkondensation. , 2013, , 1041-1046.		0
169	Verbrennungsdiagnostik über Laser-Streulicht-Verfahren. , 1992, , 15-21.		0
170	J3 Tropfenkondensation. Springer Reference Technik, 2019, , 1131-1137.	0.0	0